HHS Public Access

Author manuscript

J Med Genet. Author manuscript; available in PMC 2017 July 19.

Published in final edited form as:

J Med Genet. 2015 December ; 52(12): 830–839. doi:10.1136/jmedgenet-2015-103316.

Mutations in human homologue of chicken *talpid3* gene (*KIAA0586*) cause a hybrid ciliopathy with overlapping features of Jeune and Joubert syndromes

May Christine V Malicdan[1,2], **Thierry Vilboux**[2,3], **Joshi Stephen**[2], **Dino Maglic**[2], **Luhe Mian**[2], **Daniel Konzman**[2], **Jennifer Guo**[2], **Deniz Yildirimli**[2], **Joy Bryant**[2], **Roxanne Fischer**[2], **Wadih M Zein**[4], **Joseph Snow**[5], **Meghana Vemulapalli**[6], **James C Mullikin**[6], **Camilo Toro**[1], **Benjamin D Solomon**[3], **John E Niederhuber**[8], **NISC Comparative Sequencing Program**[6], **William A Gahl**[1,2,7], and **Meral Gunay-Aygun**[2,7]

[1]NIH Undiagnosed Diseases Program, Common Fund, Office of the Director, National Institutes of Health, Bethesda, Maryland, USA

[2]Medical Genetics Branch, National Human Genome Research Institute, National Institutes of Health, Bethesda, Maryland, USA

[3]Division of Medical Genomics, Inova Translational Medicine Institute, Falls Church, Virginia, USA

[4]Ophthalmic Genetics & Visual Function Branch, National Eye Institute, National Institutes of Health, Bethesda, Maryland, USA

Correspondence to Dr Meral Gunay-Aygun, National Human Genome Research Institute, National Institutes of Health, 10 Center Dr, Bldg 10, Rm 10C103C, Bethesda, MD 20892-1851, USA; mgaygun@mail.nih.gov.
MCVM, TV, JSt, WAG and MG-A contributed equally.

Competing interests
None declared.

Patient consent
Obtained.

Ethics approval
Institutional Review Board of the National Human Genome Research Institute, National Institutes of Health.

Provenance and peer review
Not commissioned; externally peer reviewed.

Contributors
MCVM performed most cell biology experiments, provided direction for the project, analysed the data, generated figures and wrote the manuscript. TV performed most molecular data experiments, analysed the data, generated figures and contributed to manuscript writing. JSt helped in molecular data experiments, analysed the data, helped generate figures and contributed to manuscript writing. DM contributed to cell culture experiments and data analysis and manuscript writing. LM contributed to cell culture experiments and data imaging and analysis and manuscript writing. DK contributed to analysis of cilia in cells and manuscript writing. JG contributed to cloning experiments, production of lentivirus and manuscript writing. DY assisted in screening for mutations in our ciliopathy cohort and contributed to manuscript writing. JB coordinated admitting the patients, gathering data from patients and contributed to manuscript writing. RF assisted in screening for mutations in our ciliopathy cohort and contributed to manuscript writing. WMZ gathered and analysed ophthalmological data from patients and contributed to manuscript writing. JSn gathered and analysed neurocognitive data from patients and contributed to manuscript writing. MV contributed to tools for data analysis and manuscript writing. JCM contributed to tools for data analysis and manuscript writing. CT gathered and analysed neurological data from patients and contributed to project direction and manuscript writing. BDS contributed to tools for data analysis and manuscript writing. JEN contributed to tools for data analysis and manuscript writing. NISC Comparative Sequencing Program performed whole exome sequencing and tools for data analysis. WAG provided direction for the project, obtained funding, guided data collection and interpretation and contributed to manuscript writing. MG-A, principal investigator of clinical trial NCT00068224, designed research, recruited patients, performed clinical and molecular data analysis, provided direction for the project and wrote the manuscript.

[5]Office of the Clinical Director, National Institute of Mental Health, National Institutes of Health, Bethesda, Maryland, USA

[6]NIH Intramural Sequencing Center (NISC), National Human Genome Research Institute, National Institutes of Health, Bethesda, Maryland, USA

[7]Office of the Clinical Director, National Human Genome Research Institute, National Institutes of Health, Bethesda, Maryland, USA

[8]Inova Translational Medicine Institute, Inova Health System, Falls Church, Virginia, USA

Abstract

Background—In chicken, loss of TALPID3 results in non-functional cilia and short-rib polydactyly syndrome. This phenotype is caused by a frameshift mutation in the chicken ortholog of the human *KIAA0586* gene, which encodes a novel coiled-coil domain protein essential for primary ciliogenesis, suggesting that *KIAA0586* can be associated with ciliopathy in human beings.

Methods—In our patients with ciliopathy (http://www.clinicaltrials.gov: NCT00068224), we have collected extensive clinical and neuroimaging data from affected individuals, and performed whole exome sequencing on DNA from affected individuals and their parents. We analysed gene expression on fibroblast cell line, and determined the effect of gene mutation on ciliogenesis in cells derived from patients.

Results—We identified biallelic mutations in the human *TALPID3* ortholog, *KIAA0586*, in six children with findings of overlapping Jeune and Joubert syndromes. Fibroblasts cultured from one of the patients with Jeune–Joubert syndrome exhibited more severe cilia defects than fibroblasts from patients with only Joubert syndrome; this difference was reflected in *KIAA0586* RNA expression levels. Rescue of the cilia defect with full-length wild type *KIAA0586* indicated a causal link between cilia formation and KIAA0586 function.

Conclusions—Our results show that biallelic deleterious mutations in *KIAA0586* lead to Joubert syndrome with or without Jeune asphyxiating thoracic dystrophy. Furthermore, our results confirm that KIAA0586/TALPID3 is essential in cilia formation in human beings, expand the *KIAA0586* phenotype to include features of Jeune syndrome and provide a pathogenetic connection between Joubert and Jeune syndromes, based on aberrant ciliogenesis.

INTRODUCTION

The chicken TALPID3 mutation, originally identified in 1964 on the basis of its eponymous limb defects,[1] disrupts transduction of sonic hedgehog activity in the limbs, the neural tube and the somites.[23] This phenotype is caused by a frame-shift mutation in the chicken ortholog of the human *KIAA0586* gene, which encodes a novel coiled-coil domain protein essential for primary ciliogenesis.[24] Hedgehog signalling is a highly conserved pathway that plays a fundamental role in animal development.[5]

Joubert syndrome is a ciliopathy characterised by distinctive midbrain and cerebellar malformations that result in the ‘molar tooth sign’ on axial brain images as well as hypotonia and developmental delay.[6] The majority of patients with Joubert syndrome also

display episodic tachypnoea or apnoea and abnormal eye movements. The term ‘Joubert syndrome and related disorders’ (JSRD) is used to describe individuals with Joubert syndrome plus other findings, including retinal dystrophy, ocular colobomas, hepatic fibrosis and fibrocystic renal disease. JSRD are a genetically heterogeneous group of ciliopathies; the 25 causative genes identified to date account for approximately 50%–70% of cases.

Jeune syndrome, also known as asphyxiating thoracic dystrophy, is a skeletal ciliopathy characterised by a small thorax due to short ribs, disproportionate short stature due to short long bones, polydactyly and renal, hepatic and retinal involvement.[7] Radiological skeletal abnormalities include cone-shaped epiphyses in the hands and feet, irregular metaphyses, decreased iliac cephalocaudal height and a trident-shaped acetabulum.[8] To date, biallelic mutations in 12 genes, including *CEP120*, *IFT80*, *DYNC2H1*, *TTC21B* and *WDR19*, have been found to cause Jeune syndrome.

Many ciliopathies, including Joubert, Bardet–Biedl and Meckel–Gruber syndromes, display genotypic and phenotypic overlap; this has not been demonstrated for patients with Joubert syndrome with *KIAA0586* mutations, however. Here we present six patients with biallelic mutations in *KIAA0586* and brain anomalies classic for Joubert syndrome, two of whom manifest a Joubert–Jeune overlap ciliopathy with the additional finding of a small thorax and respiratory problems.

MATERIALS AND METHODS

Patients

Patients and parents were evaluated at the National Institutes of Health (NIH) Clinical Center and enrolled in the NIH protocol ‘Clinical and Molecular Investigations into Ciliopathies’ (http://www.clinicaltrials.gov, trial NCT00068224), approved by the Institutional Review Board of the National Human Genome Research Institute (NHGRI). The parents gave written, informed consent. Evaluations at the NIH Clinical Center included family history and physical examination and comprehensive biochemical and imaging studies.

Imaging

All patients underwent axial, coronal and sagittal T1-weighted or T2-weighted brain MRI imaging at their local hospitals as part of their routine diagnostic evaluation. All available brain MRI studies were retrospectively evaluated for infratentorial and supratentorial abnormalities as previously reported.[7] Cerebellar dysplasia was defined as an abnormal cerebellar foliation, fissuration and white matter arborisation. Standard and high-resolution ultrasonographic studies were performed using 4 and 7 Mhz transducers (AVI Sequoia, Mountain View, California, USA).

The images were reviewed by two paediatric neuroradiologists, an adult neuroradiologist, a geneticist and a paediatric neurologist with high expertise in cerebellar malformations.

Sequencing and variant analysis

For exome sequencing, we used the HiSeq2000 (Illumina)[8] that employed 101 bp paired-end read sequencing. Image analysis and base calling were performed using Illumina Genome Analyzer Pipeline software V.1.13.48.0 with default parameters. Reads were aligned to a human reference sequence (UCSC assembly hg19, NCBI build 37) using a package called Efficient Large-scale Alignment of Nucleotide Databases (Illumina, San Diego, California, USA). Genotypes were called at all positions where there were high-quality sequence bases using a Bayesian algorithm called the Most Probable Genotype,[9] and variants were filtered using the graphical software tool VarSifter V.1.5.[10] The database dbSNP (http://www.ncbi.nlm.nih.gov/snp/) covers the 1.22% of the human genome corresponding to the Consensus Conserved Domain Sequences and more than 1000 non-coding RNAs.[11] BAM files of the subjects were visualised using Integrative Genomics Viewer (Broad Institute).

For dideoxy sequencing, primers were designed to cover all coding exons and flanking intronic regions of *KIAA0586* (primer sequences available on request). Direct sequencing of the PCR amplification products was carried out using BigDye V.3.1 Terminator chemistry (Applied Biosystems) and separated on an ABI 3130xl genetic analyser (Applied Biosystems). Data were evaluated using Sequencher V.5.0 software (Gene Codes, Ann Arbor, Michigan, USA).

Cell culture

Fibroblasts were cultured from forearm skin biopsies and grown in high-glucose (4.5 g/L) DMEM supplemented with 15% FBS, 2 mM L-glutamine, non-essential amino acid solution and penicillin-streptomycin. For control, normal adult human dermal fibroblasts (ATCC PCS-201-012) were used.

Expression studies

Total RNA was isolated from fibroblasts with RNeasy Mini kit (Qiagen, Valencia, California, USA)[12] and from whole blood using PAXgene Blood RNA Kit. RNA was treated with a DNase kit (DNA-free) according to the manufacturer's protocol (Applied Biosystems, Austin, Texas, USA). RNA concentration and purity were assessed on a Qubit Fluorometer (Life Technologies). First strand cDNA was synthesised using a high-capacity RNA-to-cDNA kit (Applied Biosystems). Human multiple tissue cDNA panels (human MTC panels I and II, and Human Fetal MT Panel) were purchased from Clontech (Clontech Laboratories, Mountain View, California, USA). Quantitative real-time PCR (qPCR) was performed using a KIAA0586 (Hs00914952_m1(Probe 1) and Hs0091496_m1 (Probe 2)), Assays-On-Demand primer-probe assays (Applied Biosystems) and a control assay for the *ACTB* gene. PCR amplifications were performed on 100 ng of cDNA using TaqMan Gene Expression Master Mix reagent (Applied Biosystems), and were carried out on an ABI PRISM 7900 HT Sequence Detection System (Applied Biosystems). Isoform analysis was made using primers as detailed in online supplementary table S1. qPCR was performed using a Bio-Rad iQ SYBR Green Supermix and qPCR machine with standard qPCR parameters to analyse the expression of *KIAA0586* isoforms compared with the control gene *POLR2A*. Results were analysed with the comparative C_T method as described.[13,14]

RT-PCR and TA cloning

RNA from patient 1 and his parents were isolated, and cDNA synthesis was performed as mentioned above. RT reaction products were diluted and amplified using specific primers (primer sequences available on request) as shown in online supplementary figure S1A (upper panel). PCR products were loaded into 2% agarose gel and visualised on ultraviolet transilluminator. In order to confirm the deletion, PCR products (from P1, P1-f and P1-m) were cloned in TOPO vector according to manufacturer's instructions. Random colonies were picked up, and the desired region was sequenced.

Immunofluorescence microscopy

Antibodies that were used in this study were: rabbit anti-ARL13B antibody (Proteintech Group, Chicago, Illinois, USA), mouse anti-gamma tubulin (clone GTU-88, Sigma), Alexa Fluor secondary donkey antirabbit and donkey antimouse antibodies (Invitrogen).

For cilia analysis, cells were grown in coverslips until 70% confluent, serum-starved for 24 h and fixed using ice-cold methanol for 10 min. After three washes in PBS, cells were blocked with 2% donkey serum and 2% BSA in PBS, and incubated in primary antibodies overnight at 4°C. After washing, samples were incubated in appropriate secondary antibodies, washed and mounted in Vectashield containing DAPI (Vector Laboratories). Cells were imaged with a Zeiss 510 META confocal laser-scanning microscope. Optical sections were collected from the xy plane and merged into maximum projection images. A total of 200 cells were analysed per cell line. Non-parametric t test was used to compare control and patient cells.

Production of lentiviral vectors and transduction of cells

cDNA encoding the full-length human *KIAA0586* (NM_001244189.1) was obtained by RT-PCR-mediated cloning, using total RNA from testes. KIAA0586 was cloned into pENTR11 vector by Seamless Cloning, and later subcloned into pLenti6.3/V5-DEST (Invitrogen) using Gateway Recombination (Invitrogen). Production of lentiviral constructs was performed by transient cotransfection of 293FT cells (ViraPower Lentiviral Expression Systems, Invitrogen), producing pLenti6.3-KIAA0586 and pLenti6.3-empty for control, and concentrated using Lenti-X Concentrator (Clontech) following manufacturer's protocol to generate high titre virus. Fibroblasts cells (control, patient 1 and 2) were transduced with viral preparations (1×10^7/mL, at an MOI of 10) diluted in fresh culture media supplemented with Polybrene (Sigma, with a final concentration of 8 μg/mL) twice over the duration of 12 h. Forty-eight hours after transduction, generation of cells stably expressing pLenti6.3-KIAA0586 was initiated by changing the culture media with selection antibiotic (Blasticidin, Invitrogen). After serial dilution and clone selection for stable cell line generation, cells were used for assays.

RESULTS

KIAA0586 mutations in patients with Jeune and Joubert syndromes

Patient 1 (figure 1A, upper panel, P1; table 1) was evaluated at the NIH Clinical Center at age 4.7 and 6.8 years. Prenatal ultrasonography showed Dandy–Walker anomaly at 22 weeks' gestation. At birth, patient 1 had respiratory distress associated with a small bell-

shaped thorax; he spent 12 weeks in a neonatal intensive care unit due to respiratory distress, central and obstructive apnoea and intermittent tachypnoea. Brain MRI was most consistent with Dandy–Walker variant with cerebellar and midbrain anomalies similar to Joubert syndrome (figure 1A1, A2), and bilateral diffuse polymicrogyria of supratentorial grey matter (figure 1A3). The infant was discharged with the diagnoses of Joubert and Jeune syndromes. He required several readmissions due to respiratory distress and hypoventilation. He had poor feeding due to oral motor dyscoordination and episodic tachypnoea, and required 100% G-tube feeding till age 6.5 years. At 6.8 years, his chest size had increased, but still remained small (circumference ~54 cm, 10th percentile). There was global developmental delay; he walked at 5.5 years, and was non-verbal at age 6.7 years. He had disproportionate short stature with relatively short extremities (figure 1A; upper panel, P1; table 1). He had bilateral fifth finger clinodactyly and overlapping toes; there was no polydactyly or syndactyly (see online supplementary figure S1A). Eye examination revealed oculomotor apraxia and limited lateral gaze bilaterally, and retinal examination was normal. Optic nerve head pallor indicating optic atrophy was noted on examination (see online supplementary figure S1B).

Patient 2 was evaluated at age 4.4 years (figure 1A, middle panel, P2; table 1). Perinatal history was uneventful. At 6 months, he required hospitalisation due to respiratory distress during a viral respiratory infection. He was noted to have a small bell-shaped chest, hypotonia and developmental delay. MRI at 18 months showed a mildly hypoplastic and dysplastic vermis (marked in circle in figure 1A4) and a molar tooth sign (figure 1A5). By 4.4 years of age, his chest size had normalised (figure 1A, middle panel, P2) and his height was within the normal range (table 1). Unlike patient 1, patient 2 had a normal cerebral cortex (figure 1A6). Eye examination showed a unilateral form fruste coloboma of the retina and subtle optic nerve head pallor bilaterally. Liver and kidney-related blood and urine chemistries were normal in both patients. Abdominal ultrasonography was normal in both patients except for mildly elevated liver echogenicity.

Exome sequencing was performed on both patients 1 and 2 and their parents. We identified two variants in *KIAA0586* (NM_001244189.1) and confirmed them using Sanger sequencing. Patient 1 had a synonymous variant inherited from his father (*KIAA0586:* c.990C>T; p.Leu330Leu), and patient 2 had a frameshifting duplication inherited from his father (*KIAA0586:* c.130dupC; p.His44Profs*8) (figure 2A). The synonymous p.Leu330Leu (exon 9) resulted in aberrant splicing leading to the loss of exon 9 (see online supplementary figure S2), as detected in RNA derived from patient-1 fibroblasts (see online supplementary figure S2A). By cloning the bands detected by amplifying regions between exon 8 and exon 10, we show that this deletion removes 154 bp at the RNA level (see online supplementary figure S2B), producing a frameshift with early termination 3 amino acids after the deletion in exon 10, and causing partial or complete loss of function. The c.130dupC (p.His44Profs*8) from patient 2 is predicted to cause an early termination. An additional analysis of the BAM files (see online supplementary figure S3) revealed a potential deletion in both families affecting multiple exons. We then designed multiple primer pairs to identify the breakpoints of this deletion by PCR and Sanger sequencing (figure 2A). This deletion, c.745-350_1288+1117del8260 bp, affects exon 8, 9 and 10, removes 544 coding bp and leads to a frameshift deletion with an early termination 3 amino acids after the deletion in exon 11.

Analysis of this deletion in 190 samples from ethnically matched unaffected controls showed that there were no alleles that were either homozygous or heterozygous (data not shown).

We then performed exome analysis on 130 samples of our multisystem ciliopathy families of unknown cause, and found compound heterozygous *KIAA0586* mutations in four additional unrelated patients with Joubert syndrome (table 2). Patient 3 was evaluated twice at ages 4.4 and 7.8 years (figure 1B, first panel, P3; table 1). He presented at 4 months with hypotonia and developmental delay. Brain MRI showed typical features of Joubert syndrome (figure 1B 1,2); cerebral cortex was unremarkable (figure 1B 3). At age 4.4, his chest size was normal, but his height was below average (height Z score was −2.06) (table 1). He had global developmental delay. Expressive speech was the most severely affected; he remained non-verbal at age 7.8 years. Patient 3 had the same multiple exon deletion present in patient 1 and patient 2, in addition to a c.428delG; p. Arg143Lysfs*4 frameshifting deletion (*KIAA0586:* c.428delG; p.Arg143Lysfs*4) that leads to an early termination.

Patient 4 (figure 1B, second panel, P4; table 1) had an unremarkable perinatal history. In early infancy, he required multiple hospital admissions due to respiratory distress in the context of a viral infection. He walked at 26 months, and had several words after 12 months, but had speech articulation problems. Brain MRI showed severely hypoplastic and dysplastic vermis (figure 1B 4 and 5) and normal cerebral cortex (figure 1B 6). Chest size and height were normal at age 4 years (figure 1B, second panel, P4; table 1). Eye examination showed unilateral form fruste retinal coloboma. Wechsler Intelligence test at NIH showed a full-scale IQ of 88.

Patient 5 (figure 1B, third panel, P5; table 1) had a prenatal ultrasonography at 15 weeks that showed a ‘cerebellar cyst’, and Dandy–Walker was suspected. Oligohydramnios was noted at 35 weeks. Postnatally, she did well without breathing or feeding problems. At 6 months, she was admitted due to respiratory distress during a viral respiratory infection. She was overweight at age 6 months; molecular genetic testing for Prader–Willi syndrome was negative. Eye examination at the NIH revealed bilateral lateral gaze palsy. Chest size was normal, but her height was below average (height Z score −2.01) (table 1).

Patient 6 (figure 1B, fourth panel, P6; table 1) was born at term. He had intermittent tachypnoea from birth to 2 years. Hypotonia and developmental delay were noted at 10 months. The cerebral cortex was normal on MRI (figure 1B 11). Beginning at age 10 years, he had four afebrile grand mal seizures responsive to carbamazepine. In addition, he had problems with behaviour, including difficulty with anger control. Eye examination showed normal acuity, but a moderately constricted visual field. Optic atrophy was noted on examination (see online supplementary figure 1B). The patient was cooperative with optical coherence tomography revealing thinning of the retinal nerve fibre layer consistent with a diagnosis of optic atrophy. Full scale IQ was 56 on Wechsler Intelligence test performed at NIH.

Patients 4, 5 and 6 had the same 1 bp deletion seen in patient 3 (table 2). In addition, patient 4 had c.1159C>T; p.Gln387* that leads to an early termination at amino acid 387. Patient 5

had c.1413-1G>C; this variant is predicted to lead to the skipping of exon 12 (Berkeley Drosophila Genome Project (BDGP), see URLs). Patient 6 had c.1120+1G>A that is predicted to lead to an insertion of 802 nucleotides (BDGP, see URLs) and likely leads to an early termination 5 amino acids after exon 9.

Expression of KIAA0586 in normal tissues and patient cells

KIAA0586 (Gene ID: 9786), also known as *TALPID3*, has several isoforms (figure 2B). The longest isoform (NM_001244189.1) consists of 34 exons, spans ~121 kb and codes for a 1644 amino acid protein (figure 2C). In GenBank, five additional isoforms have been described. Interestingly, all our mutations are found before the highly conserved domain of KIAA0586 that is necessary for centrosome localisation (figure 2C). Although all seven different mutations identified in our cohort are potentially deleterious alleles, they do not affect all of the six known isoforms (see online supplementary table S2).

KIAA0586 is ubiquitously expressed in various tissues (figure 3A). Of note, however, is the difference in the levels of expression using two different probes that presumably amplify common areas in all known isoforms, suggesting that there may be other isoforms that have not yet been identified. We then looked at the effect of the mutations on the transcript level by measuring *KIAA0586* mRNA transcripts of the three main coding isoforms, NM_014749.3, NM_001244189.1 and NM_001244190.1, using qPCR analysed with the comparative C_T method. In fibroblasts of patient 1 (with Jeune–Joubert syndrome) and patient 3 (with Joubert syndrome), these three isoforms were markedly reduced compared with control (figure 3B), presumably due to nonsense-mediated decay. Interestingly, a greater reduction of *KIAA0586* expression was seen in patient 1, indicating that this combination of variants is more severe or that the patients possess a modifier that affects *KIAA0586* expression.

Patients with *KIAA0586* mutations show reduced cilia length in primary fibroblasts

Therefore, using cilia-specific antibodies and immunofluorescence microscopy, we examined the ability of primary fibroblasts from patients 1 and 3 to form normal cilia. After 48 h of serum starvation, up to 80% of control cells were ciliated, while only 30% of patient-1 cells and 50% of patient 3 cells were ciliated (figure 4A). Cilia length was markedly reduced in both patients 1 and 3 (figure 4A). Transduction of cells with the full length *KIAA0586* using lentiviral-mediated system rescued the number of ciliated cells and the cilia length in both patients 1 and 3 (figure 4B). The impaired cilia formation in the cells of patients 1 and 3 supports the prediction that the deleterious variants found in our cohort disrupt the well-conserved domain of KIAA0586 that is necessary for centriole assembly and, consequently, cilia formation.

DISCUSSION

KIAA0586 plays a key role in cilia assembly[15,16] in both cellular and animal models.[17] Mutant mouse[18] and zebrafish[17] embryos lacking Kiaa0586 do not have primary cilia, and like *talpid*^{3} mutant chicken embryos, have face and neural tube defects. Mice and zebrafish that lack Kiaa0586, however, also have defects in left-right asymmetry.[17,18] KIAA0586 is a

component of a CP110-containing protein complex important for centrosome and cilia function.[19] KIAA0586 assembles a ring-like structure at the extreme distal end of centrioles. Ablation of TALPID3 results in an aberrant distribution of centriolar satellites involved in protein trafficking to centrosomes; it also causes ciliary vesicle formation reminiscent of loss of Cep290, another CP110-associated protein that is mutated in various human ciliopathies[1920] and leads to failure of centrosome migration.[20] A similar failure of centrosome positioning and/or docking is seen in cells lacking function in other genes encoding basal body proteins, including OFD1 (oral-facialdigital syndrome 1)[21] and MKS1 (Meckel syndrome 1).[22]

Although patients with Joubert with *KIAA0586* mutations have not been reported with findings of Jeune syndrome,[23] there are other precedents for the coexistence of clinical characteristics of Joubert and Jeune syndromes. The chicken talpid[3] mutant displayed a small chest and developed extremely short limbs with increased number of digits, many of which were morphologically identical.[1] In human beings, mutations in CSPP1, a spindle pole-associated protein like KIAA0586, involved in the centrosome, were recently identified in patients with Joubert syndrome with features of Jeune syndrome.[2425] Finally, the product of *CEP120*, mutated in some patients with Jeune syndrome,[23] interacts with KIAA0586.[26] In mice, the localisation of Cep120 to daughter centrioles[27] is dependent on Talpid3.[26] This interaction may explain why the phenotypes observed in our patients ranged from Jeune to Joubert syndrome.

Similar to the findings of Alby *et al*,[28] which were published while our paper was under review, our patients with *KIAA0586* mutations show reduced number of ciliated cells in fibroblasts. It is important, however, to note that the effect on cilia formation is more profound in patient 1, whose expression of *KIAA0586* at the RNA level is much more reduced as compared with patient 3. Measurement of the KIAA0586 protein levels may help clarify the issue in the future. In addition to the lack of cilia formation, we have also shown that the length of cilia in our patients' fibroblasts are much shorter when compared with control; this finding may only be specific to human fibroblasts, as TALPID3/Talpid3 deficiency in various animal models show absence of cilia formation.

Multiple deleterious alleles or variants that are predicted to produce premature stop codon have been identified in *KIAA0586* and reported in various databases (see online supplementary table S3).[28–30] However, a discrepancy arises between the high frequency of these deleterious alleles (estimated prevalence 1/3500 in Exome Variant Server and 1/30 000 in Exome Aggregation Consortium; see URLs), and the actual prevalence of Joubert syndrome, estimated at 1:100 000.[6] This may be related to the existence of multiple isoforms of *KIAA0586*, or to embryonic lethality of biallelic mutations. Also of note is the difference in severity of symptoms between patients as exemplified by patient 1 who exhibited a more severe presentation than other subjects. This again could be explained by the profound reduction in *KIAA0586* expression in cells, or the differential effect of mutations in the various *KIAA0586* isoforms. This may also explain why the phenotypes of patients with mutations in *KIAA0586* reported to this date appear to have a wide range of severity.[28–30] Further studies will be required to determine the effect of *KIAA0586* variants on the different isoforms.

Our results confirm that KIAA0586/TALPID3 is essential in cilia formation in human beings, expand the *KIAA0586* phenotype to include features of Jeune syndrome and provide a pathogenetic connection between Joubert and Jeune syndromes, based on aberrant ciliogenesis.

Supplementary Material

Refer to Web version on PubMed Central for supplementary material.

Acknowledgments

This research was supported by the Intramural Research Programs of the National Human Genome Research Institute, National Eye Institute and the National Institute of Mental Health of the National Institutes of Health, Bethesda, Maryland, USA. We also thank the patients and their families for participating in this study.

Funding

This research was supported by the Intramural Research Programs of the National Human Genome Research Institute, National Eye Institute and the National Institute of Mental Health of the National Institutes of Health, Bethesda, Maryland, USA.

References

1. Ede DA, Kelly WA. Developmental abnormalities in the trunk and limbs of the talpid3 mutant of the fowl. J Embryol Exp Morphol. 1964; 12:339–56. [PubMed: 14192055]
2. Davey MG, Paton IR, Yin Y, Schmidt M, Bangs FK, Morrice DR, Smith TG, Buxton P, Stamataki D, Tanaka M, Munsterberg AE, Briscoe J, Tickle C, Burt DW. The chicken talpid3 gene encodes a novel protein essential for Hedgehog signaling. Genes Dev. 2006; 20:1365–77. [PubMed: 16702409]
3. Lewis KE, Drossopoulou G, Paton IR, Morrice DR, Robertson KE, Burt DW, Ingham PW, Tickle C. Expression of ptc and gli genes in talpid3 suggests bifurcation in Shh pathway. Development. 1999; 126:2397–407. [PubMed: 10225999]
4. Yin YL, Bangs F, Paton IR, Prescott A, James J, Davey MG, Whitley P, Genikhovich G, Technau U, Burt DW, Tickle C. The Talpid3 gene (KIAA0586) encodes a centrosomal protein that is essential for primary cilia formation. Development. 2009; 136:655–64. [PubMed: 19144723]
5. Briscoe J, Therond PP. The mechanisms of Hedgehog signalling and its roles in development and disease. Nat Rev Mol Cell Biol. 2013; 14:416–29. [PubMed: 23719536]
6. Romani M, Micalizzi A, Valente EM. Joubert syndrome: congenital cerebellar ataxia with the molar tooth. Lancet Neurol. 2013; 12:894–905. [PubMed: 23870701]
7. Poretti A, Hausler M, von Moers A, Baumgartner B, Zerres K, Klein A, Aiello C, Moro F, Zanni G, Santorelli FM, Huisman TA, Weis J, Valente EM, Bertini E, Boltshauser E. Ataxia, intellectual disability, and ocular apraxia with cerebellar cysts: a new disease? Cerebellum. 2014; 13:79–88. [PubMed: 24013853]
8. Bentley DR, Balasubramanian S, Swerdlow HP, Smith GP, Milton J, Brown CG, Hall KP, Evers DJ, Barnes CL, Bignell HR, Boutell JM, Bryant J, Carter RJ, Keira Cheetham R, Cox AJ, Ellis DJ, Flatbush MR, Gormley NA, Humphray SJ, Irving LJ, Karbelashvili MS, Kirk SM, Li H, Liu X, Maisinger KS, Murray LJ, Obradovic B, Ost T, Parkinson ML, Pratt MR, Rasolonjatovo IM, Reed MT, Rigatti R, Rodighiero C, Ross MT, Sabot A, Sankar SV, Scally A, Schroth GP, Smith ME, Smith VP, Spiridou A, Torrance PE, Tzonev SS, Vermaas EH, Walter K, Wu X, Zhang L, Alam MD, Anastasi C, Aniebo IC, Bailey DM, Bancarz IR, Banerjee S, Barbour SG, Baybayan PA, Benoit VA, Benson KF, Bevis C, Black PJ, Boodhun A, Brennan JS, Bridgham JA, Brown RC, Brown AA, Buermann DH, Bundu AA, Burrows JC, Carter NP, Castillo N, Chiara ECM, Chang S, Neil Cooley R, Crake NR, Dada OO, Diakoumakos KD, Dominguez-Fernandez B, Earnshaw DJ, Egbujor UC, Elmore DW, Etchin SS, Ewan MR, Fedurco M, Fraser LJ, Fuentes Fajardo KV, Scott Furey W, George D, Gietzen KJ, Goddard CP, Golda GS, Granieri PA, Green DE, Gustafson DL,

Hansen NF, Harnish K, Haudenschild CD, Heyer NI, Hims MM, Ho JT, Horgan AM, Hoschler K, Hurwitz S, Ivanov DV, Johnson MQ, James T, Huw Jones TA, Kang GD, Kerelska TH, Kersey AD, Khrebtukova I, Kindwall AP, Kingsbury Z, Kokko-Gonzales PI, Kumar A, Laurent MA, Lawley CT, Lee SE, Lee X, Liao AK, Loch JA, Lok M, Luo S, Mammen RM, Martin JW, McCauley PG, McNitt P, Mehta P, Moon KW, Mullens JW, Newington T, Ning Z, Ling Ng B, Novo SM, O'Neill MJ, Osborne MA, Osnowski A, Ostadan O, Paraschos LL, Pickering L, Pike AC, Chris Pinkard D, Pliskin DP, Podhasky J, Quijano VJ, Raczy C, Rae VH, Rawlings SR, Chiva Rodriguez A, Roe PM, Rogers J, Rogert Bacigalupo MC, Romanov N, Romieu A, Roth RK, Rourke NJ, Ruediger ST, Rusman E, Sanches-Kuiper RM, Schenker MR, Seoane JM, Shaw RJ, Shiver MK, Short SW, Sizto NL, Sluis JP, Smith MA, Ernest Sohna Sohna J, Spence EJ, Stevens K, Sutton N, Szajkowski L, Tregidgo CL, Turcatti G, Vandevondele S, Verhovsky Y, Virk SM, Wakelin S, Walcott GC, Wang J, Worsley GJ, Yan J, Yau L, Zuerlein M, Mullikin JC, Hurles ME, McCooke NJ, West JS, Oaks FL, Lundberg PL, Klenerman D, Durbin R, Smith AJ. Accurate whole human genome sequencing using reversible terminator chemistry. Nature. 2008; 456:53–9. [PubMed: 18987734]

9. Teer JK, Mullikin JC. Exome sequencing: the sweet spot before whole genomes. Hum Mol Genet. 2010; 19(R2):R145–51. [PubMed: 20705737]
10. Teer JK, Green ED, Mullikin JC, Biesecker LG. VarSifter: visualizing and analyzing exome-scale sequence variation data on a desktop computer. Bioinformatics. 2012; 28:599–600. [PubMed: 22210868]
11. Gnirke A, Melnikov A, Maguire J, Rogov P, LeProust EM, Brockman W, Fennell T, Giannoukos G, Fisher S, Russ C, Gabriel S, Jaffe DB, Lander ES, Nusbaum C. Solution hybrid selection with ultra-long oligonucleotides for massively parallel targeted sequencing. Nat Biotechnol. 2009; 27:182–9. [PubMed: 19182786]
12. Cullinane AR, Vilboux T, O'Brien K, Curry JA, Maynard DM, Carlson-Donohoe H, Ciccone C, Markello TC, Gunay-Aygun M, Huizing M, Gahl WA. Homozygosity mapping and whole-exome sequencing to detect SLC45A2 and G6PC3 mutations in a single patient with oculocutaneous albinism and neutropenia. J Invest Dermatol. 2011; 131:2017–25. [PubMed: 21677667]
13. Livak, K. ABI Prism 7700 Sequence Detection System. 1997. Comparative Ct method. User bulletin #2:11-15. PE Applied Biosystems
14. Livak KJ, Schmittgen TD. Analysis of relative gene expression data using real-time quantitative PCR and the 2(−Delta Delta C(T)) Method. Methods. 2001; 25:402–8. [PubMed: 11846609]
15. Davey MG, James J, Paton IR, Burt DW, Tickle C. Analysis of talpid3 and wild-type chicken embryos reveals roles for Hedgehog signalling in development of the limb bud vasculature. Dev Biol. 2007; 301:155–65. [PubMed: 16959240]
16. Davey MG, McTeir L, Barrie AM, Freem LJ, Stephen LA. Loss of cilia causes embryonic lung hypoplasia, liver fibrosis, and cholestasis in the talpid3 ciliopathy mutant. Organogenesis. 2014; 10:177–85. [PubMed: 24743779]
17. Ben J, Elworthy S, Ng ASM, van Eeden F, Ingham PW. Targeted mutation of the talpid3 gene in zebrafish reveals its conserved requirement for ciliogenesis and Hedgehog signalling across the vertebrates. Development. 2011; 138:4969–78. [PubMed: 22028029]
18. Bangs F, Antonio N, Thongnuek P, Welten M, Davey MG, Briscoe J, Tickle C. Generation of mice with functional inactivation of talpid3, a gene first identified in chicken. Development. 2011; 138:3261–72. [PubMed: 21750036]
19. Kobayashi T, Kim S, Lin YC, Inoue T, Dynlacht BD. The CP110-interacting proteins Talpid3 and Cep290 play overlapping and distinct roles in cilia assembly. J Cell Biol. 2014; 204:215–29. [PubMed: 24421332]
20. Stephen LA, Davis GM, Mcteir KE, James J, Mcteir L, Kierans M, Bain A, Davey MG. Failure of centrosome migration causes a loss of motile cilia in talpid(3) mutants. Dev Dynam. 2013; 242:923–31.
21. Singla V, Romaguera-Ros M, Garcia-Verdugo JM, Reiter JF. Ofd1, a human disease gene, regulates the length and distal structure of centrioles. Dev Cell. 2010; 18:410–24. [PubMed: 20230748]
22. Dawe HR, Smith UM, Cullinane AR, Gerrelli D, Cox P, Badano JL, Blair-Reid S, Sriram N, Katsanis N, Attie-Bitach T, Afford SC, Copp AJ, Kelly DA, Gull K, Johnson CA. The Meckel-

Gruber Syndrome proteins MKS1 and meckelin interact and are required for primary cilium formation. Hum Mol Genet. 2007; 16:173–86. [PubMed: 17185389]

23. Shaheen R, Schmidts M, Faqeih E, Hashem A, Lausch E, Holder I, Superti-Furga A, Mitchison HM, Almoisheer A, Alamro R, Alshiddi T, Alzahrani F, Beales PL, Alkuraya FS. Consortium UK. A founder CEP120 mutation in Jeune asphyxiating thoracic dystrophy expands the role of centriolar proteins in skeletal ciliopathies. Hum Mol Genet. 2015; 24:1410–19. [PubMed: 25361962]
24. Lehman AM, Eydoux P, Doherty D, Glass IA, Chitayat D, Chung BY, Langlois S, Yong SL, Lowry RB, Hildebrandt F, Trnka P. Co-occurrence of Joubert syndrome and Jeune asphyxiating thoracic dystrophy. Am J Med Genet A. 2010; 152A:1411–19. [PubMed: 20503315]
25. Tuz K, Bachmann-Gagescu R, O'Day DR, Hua K, Isabella CR, Phelps IG, Stolarski AE, O'Roak BJ, Dempsey JC, Lourenco C, Alswaid A, Bonnemann CG, Medne L, Nampoothiri S, Stark Z, Leventer RJ, Topcu M, Cansu A, Jagadeesh S, Done S, Ishak GE, Glass IA, Shendure J, Neuhauss SCF, Haldeman-Englert CR, Doherty D, Ferland RJ. Mutations in CSPP1 cause primary cilia abnormalities and Joubert syndrome with or without Jeune asphyxiating thoracic dystrophy (vol 94, pg 62, 2014). Am J Hum Genet. 2014; 94:310.
26. Wu C, Yang M, Li J, Wang C, Cao T, Tao K, Wang B. Talpid3-binding centrosomal protein Cep120 is required for centriole duplication and proliferation of cerebellar granule neuron progenitors. PLoS ONE. 2014; 9:e107943. [PubMed: 25251415]
27. Mahjoub MR, Xie Z, Stearns T. Cep120 is asymmetrically localized to the daughter centriole and is essential for centriole assembly. J Cell Biol. 2010; 191:331–46. [PubMed: 20956381]
28. Alby C, Piquand K, Huber C, Megarbane A, Ichkou A, Legendre M, Pelluard F, Encha-Ravazi F, Tayeh GA, Bessieres B, El Chehadeh-Djebbar S, Laurent N, Faivre L, Sztriha L, Zombor M, Szabo H, Failler M, Garfa-Traore M, Bole C, Nitschke P, Nizon M, Elkhartoufi N, Clerget-Darpoux F, Munnich A, Lyonnet S, Vekemans M, Cormier-Daire V, Attie-Bitach T, Thomas S. Mutations in KIAA0586 cause lethal ciliopathies ranging from a hydrolethalus phenotype to short-rib polydactyly syndrome. Am J Hum Genet. 2015; 97:311–18. [PubMed: 26166481]
29. Roosing S, Hofree M, Kim S, Scott E, Copeland B, Romani M, Silhavy JL, Rosti RO, Schroth J, Mazza T, Miccinilli E, Zaki MS, Swoboda KJ, Milisa-Drautz J, Dobyns WB, Mikati MA, Incecik F, Azam M, Borgatti R, Romaniello R, Boustany RM, Clericuzio CL, D'Arrigo S, Stromme P, Boltshauser E, Stanzial F, Mirabelli-Badenier M, Moroni I, Bertini E, Emma F, Steinlin M, Hildebrandt F, Johnson CA, Freilinger M, Vaux KK, Gabriel SB, Aza-Blanc P, Heynen-Genel S, Ideker T, Dynlacht BD, Lee JE, Valente EM, Kim J, Gleeson JG. Functional genome-wide siRNA screen identifies KIAA0586 as mutated in Joubert syndrome. Elife. 2015; 4:e06602. [PubMed: 26026149]
30. Bachmann-Gagescu R, Phelps IG, Dempsey JC, Sharma VA, Ishak GE, Boyle EA, Wilson M, Marques Lourenco C, Arslan M, Shendure J, Doherty D. University of Washington Center for Mendelian G. KIAA0586 is mutated in Joubert syndrome. Hum Mutat. 2015; 36:831–5. [PubMed: 26096313]

URLs

- BDGP (http://www.fruitfly.org/cgi-bin/seq_tools/splice.pl)
- Exome Aggregation Consortium (http://exac.broadinstitute.org)
- Exome Variant Server (http://evs.gs.washington.edu/EVS/)
- dbSNP (http://www.ncbi.nlm.nih.gov/SNP/)
- GenBank (http://www.ncbi.nlm.nih.gov/genbank/)

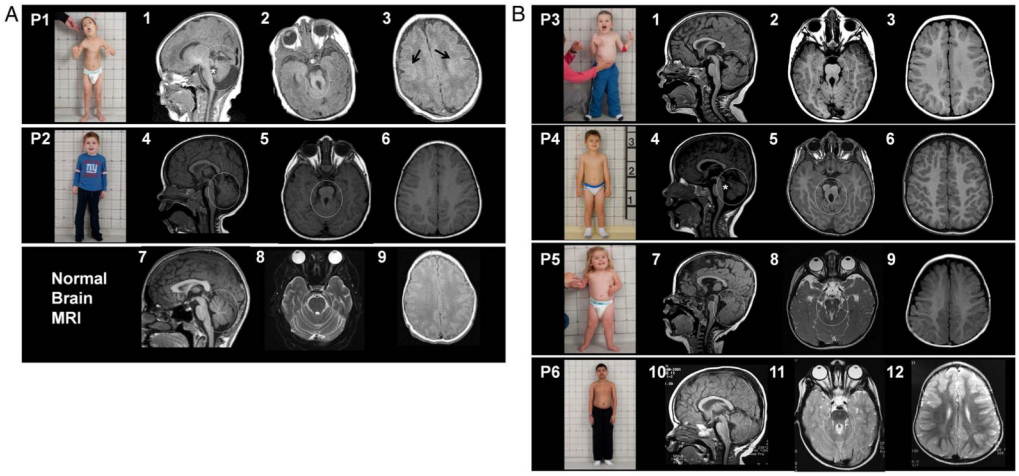

Figure 1.

Clinical photographs and imaging of subjects with Jeune–Joubert syndrome and Joubert syndrome. (A) Upper panel shows photograph of patient 1 (P1) with small thorax, relatively long trunk and short extremities, and craniofacial dysmorphism, including low set incompletely rotated ears, hypoplastic midface, epicanthal folds and lower lip scars due to biting. Brain MRI performed on the third day of life showing severe cerebellar vermis hypoplasia and dysplasia, marked retrocerebellar fluid (circle) and enlarged fourth ventricle with abnormal shape (asterisk) in (1); thickened superior cerebellar peduncles with abnormally oblique orientation resulting in the 'molar tooth sign' (circle) in (2) and cerebral cortex showing bilateral diffuse polymicrogyria (arrows) in (3). Middle panel shows photograph of patient 2 (P2) with normalised chest size at age 4.4 years; his chest was small and bell-shaped during the first year of life. Brain MRI at 18 months showing a mildly hypoplastic and dysplastic vermis (circle) in (4) and molar tooth sign (circle) in (5) and normal cerebral cortex (6). Lower panels show normal brain MRI images for comparison (7, 8 and 9). (B) First panel shows photograph of patient 3 (P3) displaying epicanthal folds, low set ears and normal chest size. Brain MRI at 2 years 4 months displaying a hypoplastic and dysplastic vermis (circle) in (1), molar tooth sign (circle) in (2) and normal cerebellar cortex (3). Second panel shows photograph of patient 4 (P4) showing normal chest size. Brain MRI of P4 at age 3 years 3 months displaying severely hypoplastic and dysplastic vermis (circle) and enlarged and abnormally shaped fourth ventricle (asterisk) in (4), molar tooth sign (5) and normal cerebral cortex (6). Third panel shows photograph of patient 5 (P5) showing a chubby 26-month-old with normal chest size. Brain MRI of P5 at age 14 months showing mildly hypoplastic and dysplastic cerebellar vermis (circle) and enlarged fourth ventricle (7), molar tooth sign (circle) in (8) and normal cerebral cortex (9). Fourth panel shows patient 6 (P6), whose chest size was normal. Brain MRI of P6 shows mildly hypoplastic and dysplastic cerebellar vermis (10, circle), enlarged fourth ventricle images, molar tooth sign (circle, in 11) and normal cerebral cortex (12).

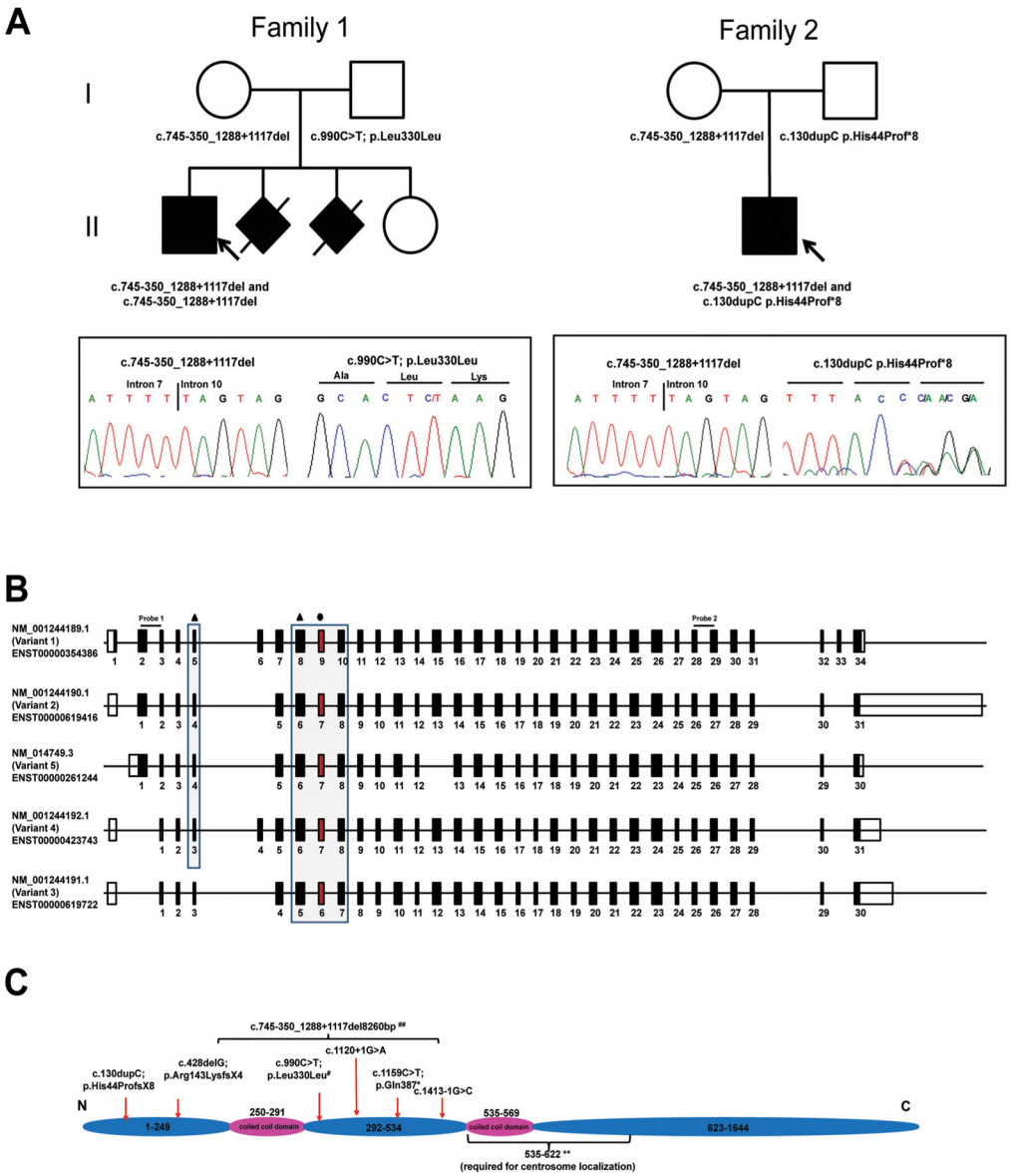

Figure 2.

Pedigree of families and molecular data. (A) Family pedigrees of patient 1 and patient 2 and representative chromatograms showing variants in *KIAA0586*. Affected individuals are shown in black, while arrows point to the probands in each family. Note that in patient 1, the c.990C>T mutation appears homozygous; patient 1 is hemizygous for this variant, as the other allele on this region is deleted due to the mutation that he inherited from his mother (c. 745-350_1288+1117del). (B) Schema showing the main isoforms of *KIAA0586*. Mutations affect most, but not all, isoforms. Black triangle refers to mutations that are predicted to produce a premature stop; black circle refers to the synonymous variant that leads to deletion of exon 9 (exon highlighted in red). Probe 1 and probe 2 refers the exons amplified for expression analysis. (C) Protein schema showing the location of mutations. All mutations are found before amino acids 535-622, a highly conserved domain required for centrosome

localisation (**, refers to the findings by Yin *et al*[4]). # refers to the synonymous variant that leads to the deletion of exon 9; ## refers to the variant that deletes exon 8, 9 and 10.

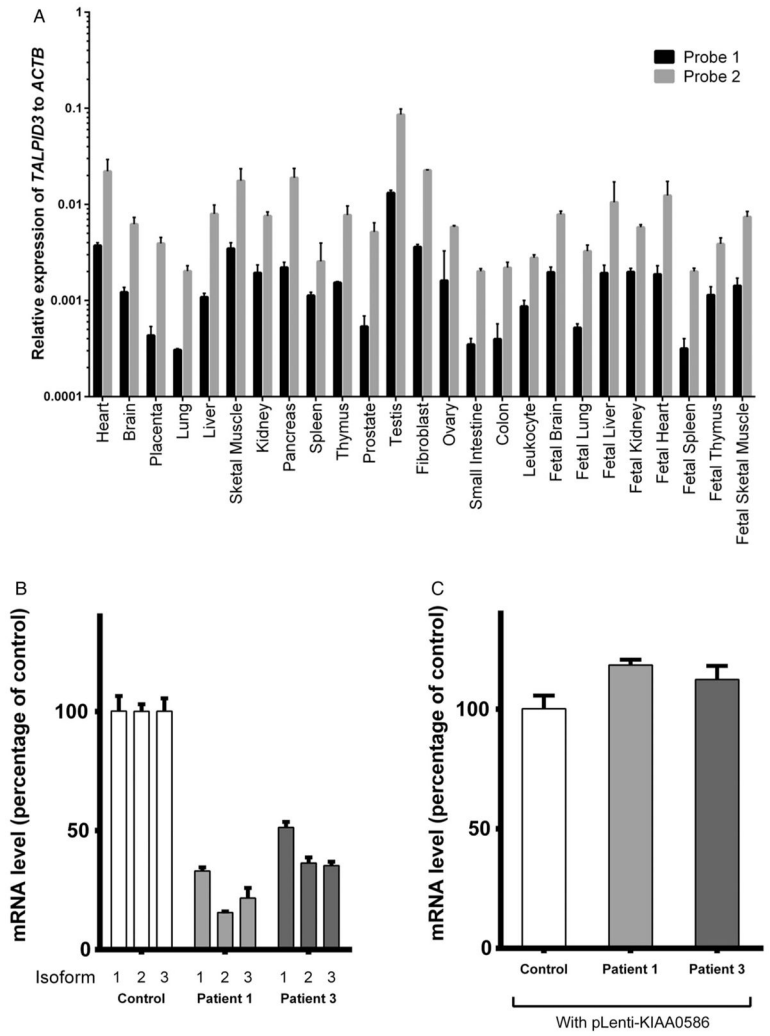

Figure 3.

Expression of *KIAA0586* in multiple tissue panel and cells. (A) Tissue expression of *KIAA0586* in multiple tissue panels from normal, unaffected individuals using two probes that amplify the first two and the last few exons of the gene, respectively (See figure 2B for probe sites). *KIAA0586* appears ubiquitously expressed, but the levels of expression vary with the two probes. (B) Analysis of common coding isoforms of KIAA0586 in affected individuals compared with unaffected control samples. mRNA was extracted from the fibroblasts of control individual (control), patient 1 (P1) and patient 3 (P3) and analysed by QPCR using primer pairs that specifically amplify the known coding isoforms of *KIAA0586* (NM_014749.3, isoform 1; NM_001244189.1, isoform 2; and NM_001244190.1, isoform 3). Expression of all three isoforms was markedly reduced in P1 and reduced by half in P3. (C) Overexpression of the full length human *KIAA0586* (NM_014749.3) in fibroblasts by lentiviral-mediated transduction led to recovery of expression in both P1 and P3. *KIAA0586* isoform expression was normalised to that of *POLR2A*.

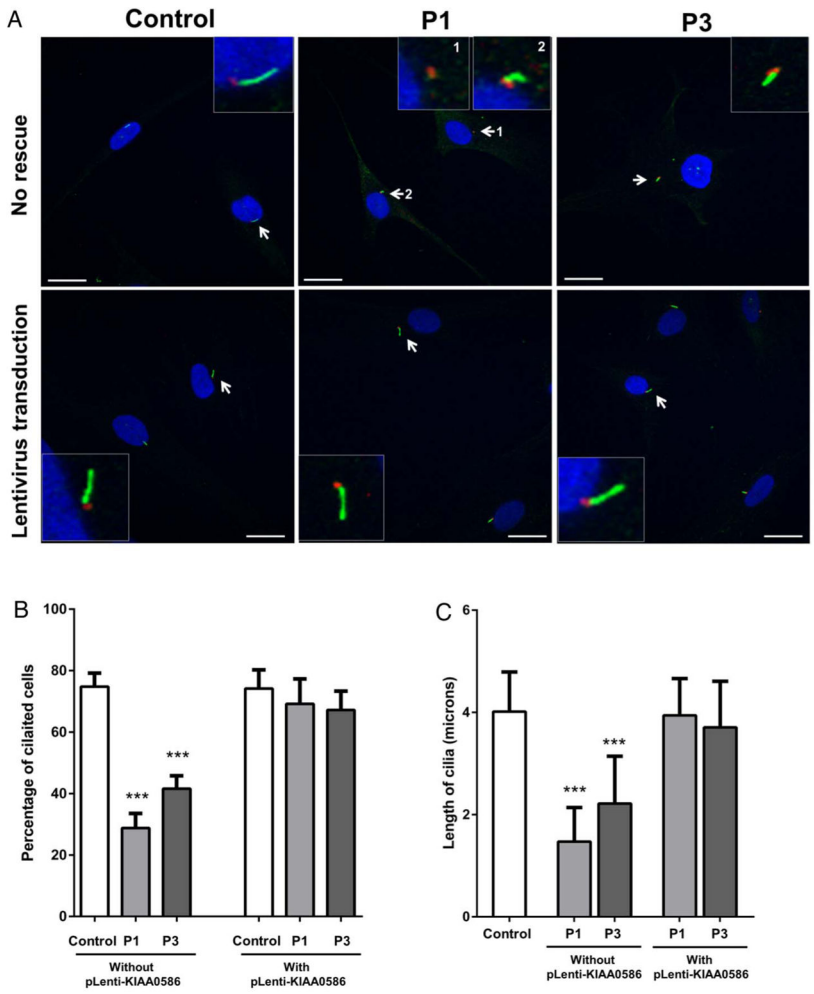

Figure 4.

Analysis of cilia in patient 1 and patient 3 with mutations in KIAA0586. (A) Fibroblasts from control, patient 1 (P1) and patient 3 (P3) were grown to near confluence and serum starved to allow formation of cilia. Forty-eight hours after serum starvation, cells were fixed in methanol and probed with anti-ARL13B antibody (green) that marks cilia and mouse antiacetylated tubulin (red) that stains the basal bodies. Insets show magnified images of cells (arrows). (B) Approximately 80% of control cells have cilia, while only 30% and 50% of cells are ciliated in P1 and P3, respectively. Overexpression of the full length human *KIAA0586* (NM_014749.3) in fibroblasts by lentiviral-mediated transduction increased the number of ciliated P1 and P3 cells to normal. Scale bars represent 20 μm. Asterisks indicate p value <0.001 between control and patient (P1 or P3) cells using non-parametric t test. (C) Cilia length in cells was measured using Zen 2009 software (Zeiss). In control cells, cilia were ~3.5–7 μ in length. In P3, the cilia length ranged from 0.05 to 2.5 μ. In P3, cells had longer cilia than P1 (without pLenti-KIAA0586), measuring 2.5–5 μ, but still shorter than control. The length of cilia in P1 and P3 cells returned to normal after transduction with full length human *KIAA0586* (with pLenti-KIAA0586). Asterisks indicate p value <0.001 between control and patient (P1 or P3) cells using non-parametric t test.

J Med Genet. Author manuscript; available in PMC 2017 July 19.

Table 1

Clinical characteristics of patients with *KIAA0586* mutations

	Jeune–Joubert syndrome		Joubert syndrome			
Characteristics	**Patient 1**	**Patient 2**	**Patient 3**	**Patient 4**	**Patient 5**	**Patient 6**
Age (years)	4.7	4.4	4.4	4	2.2	13.6
Hypertelorism	–	–	–	–	–	–
Retinal coloboma	–	Unilateral, form fruste	–	Unilateral, form fruste	–	–
Retina	–	–	–	–	–	–
Oculomotor apraxia	+	+	+	+	+	–
Strabismus/extraocular eye movements	Bilateral lateral gaze palsy	–	–	+	Bilateral lateral gaze palsy	Yes
Ptosis	–	–	–	–	–	–
Kidney function (GFR*)	102	88	122	114	N	126
Optic nerve pallor/atrophy	+	Subtle	–	+	–	+
Kidney ultrasonography	N	N	N	N	N	N
Liver enzymes	N	N	N	N	N	N
Liver echogenicity on ultrasonography	Mildly ↑	Mildly ↑	Normal	Mildly ↑	Mildly ↑	Normal
Spleen length:height ratio†	0.62	0.7	0.72	0.61	0.89	0.59
Portal hypertension	–	–	–	–	–	–
Polydactyly	–	–	–	–	–	–
Height Z score	−2.13	0.49	−2.06	1.43	−2.01	−1.24
Short stature	+	–	+	–	+	–
Small chest	Yes, respiratory distress 0–2 months	Yes, normalised after 18 months	–	–	–	–
Epilepsy	–	–	–	–	–	Yes
Cerebral grey matter anomaly	Diffuse polymicrogyria	–	–	–	–	–
Neurodevelopmental function‡	Composite score of 58 and Picture Vocabulary of 46 at 4.7 years, walked at 5.5 years, non-verbal at 8 years	Walked at 2 years, 2-word phrases at age 2 years	Vineland-II Composite score 64 and Picture Vocabulary of 85 at 4.4 years, non-verbal at 8 years	FSIQ score 88, Vineland Composite score 87 at 4 years, walked, single words at 26 months	Vineland-II Composite score 78 at 5 years, 30 words, no 2-word phrases	FSIQ score 56 at 13.6 years, walked at 27 months, 2-word phrases at 2.5 years

Clinical features of individuals with *KIAA0586* mutations in our cohort with Jeune–Joubert and Joubert syndromes. N, normal; —, no information available.

*GFR, glomerular filtration rate, in ml/min/1.83 m^2.

[†]Spleen length:height ratio is a measure of portal hypertension.

[≠]The Vineland-II is a semistructured parental interview, which produces a composite score reflecting patients' adaptive functioning, including communication, socialisation, motor and daily living skills. An age-appropriate Wechsler intelligence test was administered to determine patients' FSIQ (full scale IQ). The Peabody Picture Vocabulary-4 was used to measure receptive language in some patients. Each of these measures (Vineland-II, Wechsler and Peabody) has a mean of 100, SD of 15.

Table 2

KIAA0586 mutations in our patients with Jeune and Joubert syndromes

	Allele 1			Allele 2		
Patient number	**Variant**	**Consequence**	**Origin**	**Variant**	**Consequence**	**Origin**
Patient 1	c.990C>T; p.Leu330Leu	Loss of exon 9, early termination	Paternal	c.745-350_1288+1117del	Loss of exons 8, 9 and 10, early termination	Maternal
Patient2	c.130dupC; p. His44Profs*8	Early termination	Paternal	c.745-350_1288+1117del	Loss of exons 8, 9 and 10, early termination	Maternal
Patient3	c.428delG; p. Arg143Lysfs*4	Early termination	Paternal (?)	c.745-350_1288+1117del	Loss of exons 8, 9 and 10, early termination	Maternal
Patient 4	c.428delG; p. Arg143Lysfs*4	Early termination	Maternal	c.1159C>T; p.Gln387*	Early termination	Paternal
Patient 5	c.428delG; p. Arg143Lysfs*4	Early termination	Maternal	c.1413-1G>C	Skipping of exon 12	Paternal
Patient 6	c.428delG; p. Arg143Lysfs*4	Early termination	Maternal	c.1120+1G>A	Early termination	Paternal (?)

Mutations nomenclature is based on GenBank: NM_001244189.1.